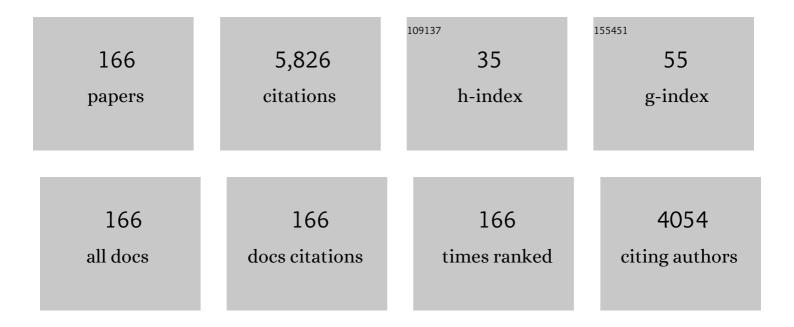
List of Publications by Year in descending order

Source: https://exaly.com/author-pdf/1564164/publications.pdf Version: 2024-02-01



#	Article	IF	CITATIONS
1	Precorneal and Pre- and Postlens Tear Film Thickness Measured Indirectly with Optical Coherence Tomography. , 2003, 44, 2524.		186
2	The TFOS International Workshop on Contact Lens Discomfort: Report of the Contact Lens Interactions With the Tear Film Subcommittee. , 2013, 54, TFOS123.		167
3	Retinal Microvascular Network and Microcirculation Assessments in High Myopia. American Journal of Ophthalmology, 2017, 174, 56-67.	1.7	162
4	Altered Macular Microvasculature in Mild Cognitive Impairment and Alzheimer Disease. Journal of Neuro-Ophthalmology, 2018, 38, 292-298.	0.4	141
5	Upper and Lower Tear Menisci in the Diagnosis of Dry Eye. , 2009, 50, 2722.		136
6	Ultra-High Resolution Optical Coherence Tomography for Differentiation of Ocular Surface Squamous Neoplasia and Pterygia. Ophthalmology, 2012, 119, 481-486.	2.5	135
7	Ultra High-Resolution Anterior Segment Optical Coherence Tomography in the Diagnosis and Management of Ocular Surface Squamous Neoplasia. Ocular Surface, 2014, 12, 46-58.	2.2	134
8	Effect of Blinking on Tear Dynamics. , 2007, 48, 3032.		130
9	Relationships between Central Tear Film Thickness and Tear Menisci of the Upper and Lower Eyelids. Investigative Ophthalmology and Visual Science, 2006, 47, 4349-4355.	3.3	127
10	Retinal Microvasculature Alteration in High Myopia. , 2016, 57, 6020.		125
11	Age-Related Alterations in the Retinal Microvasculature, Microcirculation, and Microstructure. , 2017, 58, 3804.		118
12	Topographical Thickness of the Epithelium and Total Cornea after Overnight Wear of Reverse-Geometry Rigid Contact Lenses for Myopia Reduction. , 2003, 44, 4742.		113
13	Repeated Measurements of Dynamic Tear Distribution on the Ocular Surface after Instillation of Artificial Tears. , 2006, 47, 3325.		110
14	Correlations Among Upper and Lower Tear Menisci, Noninvasive Tear Break-up Time, and the Schirmer Test. American Journal of Ophthalmology, 2008, 145, 795-800.e1.	1.7	110
15	Use of Ultra-High-Resolution Optical Coherence Tomography to Detect In Vivo Characteristics of Descemet's Membrane in Fuchs' Dystrophy. Ophthalmology, 2010, 117, 1220-1227.	2.5	104
16	The measurement of corneal epithelial thickness in response to hypoxia using optical coherence tomography11Proprietary interests: The authors have no proprietary interest in any materials or methods described within this article American Journal of Ophthalmology, 2002, 133, 315-319.	1.7	100
17	Noncontact Measurements of Central Corneal Epithelial and Flap Thickness after Laser In Situ Keratomileusis. , 2004, 45, 1812.		94
18	Diagnosis and Management of Conjunctival and Corneal Intraepithelial Neoplasia Using Ultra High-Resolution Optical Coherence Tomography. Ophthalmology, 2011, 118, 1531-1537.	2.5	90

#	Article	IF	CITATIONS
19	Diagnosis of Ocular Surface Lesions Using Ultra–High-Resolution Optical Coherence Tomography. Ophthalmology, 2013, 120, 883-891.	2.5	86
20	Retinal Microvascular Impairment in the Early Stages of Parkinson's Disease. , 2018, 59, 4115.		86
21	Ultrahigh-Resolution Measurement by Optical Coherence Tomography of Dynamic Tear Film Changes on Contact Lenses. , 2010, 51, 1988.		81
22	Topographic Thickness of Bowman's Layer Determined by Ultra-High Resolution Spectral Domain–Optical Coherence Tomography. , 2011, 52, 3901.		78
23	Diurnal Variation of Upper and Lower Tear Menisci. American Journal of Ophthalmology, 2008, 145, 801-806.e2.	1.7	73
24	Zwitterion-functionalized dendrimer-entrapped gold nanoparticles for serum-enhanced gene delivery to inhibit cancer cell metastasis. Acta Biomaterialia, 2019, 99, 320-329.	4.1	71
25	Lower Volumes of Tear Menisci in Contact Lens Wearers with Dry Eye Symptoms. , 2009, 50, 3159.		66
26	MiR-206 suppresses epithelial mesenchymal transition by targeting TGF-β signaling in estrogen receptor positive breast cancer cells. Oncotarget, 2016, 7, 24537-24548.	0.8	66
27	Ultra-High Resolution Optical Coherence Tomography for Imaging the Anterior Segment of the Eye. Ophthalmic Surgery Lasers and Imaging Retina, 2011, 42, S15-27.	0.4	66
28	Age-Related Alterations in Retinal Tissue Perfusion and Volumetric Vessel Density. , 2019, 60, 685.		60
29	Relation between optical coherence tomography and optical pachymetry measurements of corneal swelling induced by hypoxia. American Journal of Ophthalmology, 2002, 134, 93-98.	1.7	59
30	In Situ Visualization of Tears on Contact Lens Using Ultra High Resolution Optical Coherence Tomography. Eye and Contact Lens, 2009, 35, 44-49.	0.8	59
31	Optical coherence tomography for ocular surface and corneal diseases: a review. Eye and Vision (London, England), 2018, 5, 13.	1.4	59
32	Anterior Segment Biometry during Accommodation Imaged with Ultralong Scan Depth Optical Coherence Tomography. Ophthalmology, 2012, 119, 2479-2485.	2.5	57
33	The Use of Bowman's Layer Vertical Topographic Thickness Map in the Diagnosis of Keratoconus. Ophthalmology, 2014, 121, 988-993.	2.5	57
34	Targeted doxorubicin delivery to hepatocarcinoma cells by lactobionic acid-modified laponite nanodisks. New Journal of Chemistry, 2015, 39, 2847-2855.	1.4	56
35	Functional slit lamp biomicroscopy for imaging bulbar conjunctival microvasculature in contact lens wearers. Microvascular Research, 2014, 92, 62-71.	1.1	54
36	Role of high resolution optical coherence tomography in diagnosing ocular surface squamous neoplasia with coexisting ocular surface diseases. Ocular Surface, 2017, 15, 688-695.	2.2	54

#	Article	IF	CITATIONS
37	Characterization of Soft Contact Lens Edge Fitting Using Ultra-High Resolution and Ultra-Long Scan Depth Optical Coherence Tomography. , 2011, 52, 4091.		53
38	Deep Retinal Capillary Plexus Decreasing Correlated With the Outer Retinal Layer Alteration and Visual Acuity Impairment in Pathological Myopia. , 2020, 61, 45.		49
39	Dynamic Distribution of Artificial Tears on the Ocular Surface. JAMA Ophthalmology, 2008, 126, 619.	2.6	47
40	Diurnal Variation of Ocular Hysteresis, Corneal Thickness, and Intraocular Pressure. Optometry and Vision Science, 2008, 85, 1185-1192.	0.6	47
41	Tear Menisci and Ocular Discomfort during Daily Contact Lens Wear in Symptomatic Wearers. , 2011, 52, 2175.		47
42	Impaired retinal microcirculation in multiple sclerosis. Multiple Sclerosis Journal, 2016, 22, 1812-1820.	1.4	46
43	Daytime Variations of Tear Osmolarity and Tear Meniscus Volume. Eye and Contact Lens, 2012, 38, 282-287.	0.8	45
44	Visualization of Focal Thinning of the Ganglion Cell–Inner Plexiform Layer in Patients with Mild Cognitive Impairment and Alzheimer's Disease. Journal of Alzheimer's Disease, 2018, 64, 1261-1273.	1.2	45
45	Effect of Blinking on Tear Volume After Instillation of Midviscosity Artificial Tears. American Journal of Ophthalmology, 2008, 146, 920-924.	1.7	41
46	Nutritional and medical food therapies for diabetic retinopathy. Eye and Vision (London, England), 2020, 7, 33.	1.4	41
47	Impaired retinal microcirculation in patients with Alzheimer's disease. PLoS ONE, 2018, 13, e0192154.	1.1	41
48	SD-OCT with Prolonged Scan Depth for Imaging the Anterior Segment of the Eye. Ophthalmic Surgery Lasers and Imaging Retina, 2010, 41, S65-9.	0.4	40
49	Whole Eye Axial Biometry During Accommodation Using Ultra-long Scan Depth Optical Coherence Tomography. American Journal of Ophthalmology, 2014, 157, 1064-1069.e2.	1.7	39
50	Vertical and Horizontal Corneal Epithelial Thickness Profiles Determined by Ultrahigh Resolution Optical Coherence Tomography. Cornea, 2012, 31, 1036-1043.	0.9	38
51	Characteristics of Retinal Structural and Microvascular Alterations in Early Type 2 Diabetic Patients. , 2018, 59, 2110.		38
52	Synthesis of glycoconjugated poly(amindoamine) dendrimers for targeting human liver cancer cells. RSC Advances, 2012, 2, 99-102.	1.7	37
53	Automated segmentation and fractal analysis of high-resolution non-invasive capillary perfusion maps of the human retina. Microvascular Research, 2013, 89, 172-175.	1.1	36
54	Simultaneous real-time imaging of the ocular anterior segment including the ciliary muscle during accommodation. Biomedical Optics Express, 2013, 4, 466.	1.5	36

ARTICLE IF CITATIONS Cochlin, Intraocular Pressure Regulation and Mechanosensing. PLoS ONE, 2012, 7, e34309. 1.1 Tear Meniscus Volume in Dry Eye after Punctal Occlusion., 2010, 51, 1965. 56 34 Characteristic of entire corneal topography and tomography for the detection of sub-clinical 1.6 34 keratoconus with Zernike polynomials using Pentacam. Scientific Reports, 2017, 7, 16486. Entire Contact Lens Imaged In Vivo and In Vitro With Spectral Domain Optical Coherence Tomography. 58 0.8 33 Eye and Contact Lens, 2010, 36, 73-76. Reduced Tear Meniscus Dynamics in Dry Eye Patients With Aqueous Tear Deficiency. American Journal of Ophthalmology, 2010, 149, 932-938.e1 Repeated Measurements of the Anterior Segment During Accommodation Using Long Scan Depth Optical Coherence Tomography. Eye and Contact Lens, 2012, 38, 102-108. 60 0.8 33 Versatile optical coherence tomography for imaging the human eye. Biomedical Optics Express, 2013, 4, 1.5 Vessel Sampling and Blood Flow Velocity Distribution With Vessel Diameter for Characterizing the 62 0.8 32 Human Bulbar Čonjunctival Microvasculature. Eye and Contact Lens, 2016, 42, 135-140. Bulbar conjunctival microvascular responses in dry eye. Ocular Surface, 2017, 15, 193-201. 2.2 Deep perifoveal vessel density as an indicator of capillary loss in high myopia. Eye, 2019, 33, 1961-1968. 1.1 31 64 Measurement variability of the bulbar conjunctival microvasculature in healthy subjects using 1.1 functional slit lamp biomicroscopy (FSLB). Microvascular Research, 2015, 101, 15-19. Upper Punctal Occlusion versus Lower Punctal Occlusion in Dry Eye., 2010, 51, 5571. 66 28 In Vivo Morphologic Characteristics of Salzmann Nodular Degeneration With Ultra-High-Resolution 28 Optical Coherence Tomography. American Journal of Ophthalmology, 2011, 151, 248-256.e2. Age-Related Changes in Tear Menisci Imaged by Optical Coherence Tomography. Optometry and Vision 68 0.6 28 Science, 2011, 88, 1214-1219. Clinical Significance of Tear Menisci in Dry Eye. Eye and Contact Lens, 2012, 38, 183-187. 69 Visual Function and Disability Are Associated with Increased Retinal Volumetric Vessel Density in 70 1.7 28 Patients with Multiple Sclerosis. American Journal of Ophthalmology, 2020, 213, 34-45. Broadband superluminescent diode–based ultrahigh resolution optical coherence tomography for 71 1.4 ophthalmic imaging. Journal of Biomedical Optics, 2011, 16, 126006. InÂVivo Characteristics of Corneal Endothelium/Descemet Membrane Complex for the Diagnosis of 72 1.7 27 Corneal Graft Rejection. American Journal of Ophthalmology, 2017, 178, 27-37.

#	Article	IF	CITATIONS
73	Relationships among retinal/choroidal thickness, retinal microvascular network and visual field in high myopia. Acta Ophthalmologica, 2020, 98, e709-e714.	0.6	27
74	Phacoemulsification Induced Transient Swelling of Corneal Descemet's Endothelium Complex Imaged with Ultra-High Resolution Optical Coherence Tomography. PLoS ONE, 2013, 8, e80986.	1.1	26
75	Value of corneal epithelial and Bowman's layer vertical thickness profiles generated by UHR-OCT for sub-clinical keratoconus diagnosis. Scientific Reports, 2016, 6, 31550.	1.6	26
76	In Vivo Structural Characteristics of the Femtosecond LASIK-Induced Opaque Bubble Layers with Ultrahigh-Resolution SD-OCT. Ophthalmic Surgery Lasers and Imaging Retina, 2010, 41, S109-13.	0.4	26
77	InÂVivo Characterization of Retinal Microvascular Network in Multiple Sclerosis. Ophthalmology, 2016, 123, 437-438.	2.5	24
78	A Mini Review of Clinical and Research Applications of the Retinal Function Imager. Current Eye Research, 2018, 43, 273-288.	0.7	24
79	Reduced macular inner retinal thickness and microvascular density in the early stage of patients with dysthyroid optic neuropathy. Eye and Vision (London, England), 2020, 7, 16.	1.4	24
80	Microvascular abnormalities in dry eye patients. Microvascular Research, 2018, 118, 155-161.	1.1	23
81	Photoreceptor Degeneration is Correlated With the Deterioration of Macular Retinal Sensitivity in High Myopia. , 2019, 60, 2800.		23
82	Corneal epithelial thickness profile in dry-eye disease. Eye, 2020, 34, 915-922.	1.1	23
83	Evaluation of a Transgenic Mouse Model of Multiple Sclerosis with Noninvasive Methods. , 2011, 52, 2405.		22
84	Human conjunctival microvasculature assessed with a retinal function imager (RFI). Microvascular Research, 2013, 85, 134-137.	1.1	22
85	Reduced Retinal Microvascular Density Related to Activity Status and Serum Antibodies in Patients with Graves' Ophthalmopathy. Current Eye Research, 2020, 45, 576-584.	0.7	22
86	Vertical and Horizontal Corneal Epithelial Thickness Profile Using Ultra-High Resolution and Long Scan Depth Optical Coherence Tomography. PLoS ONE, 2014, 9, e97962.	1.1	21
87	Neurostimulation of the Lacrimal Nerve for Enhanced Tear Production. Ophthalmic Plastic and Reconstructive Surgery, 2015, 31, 145-151.	0.4	21
88	Retinal tissue hypoperfusion in patients with clinical Alzheimer's disease. Eye and Vision (London,) Tj ETQq	0000rgBT/	Overlock 10
89	Automatic Segmentation of the Central Epithelium Imaged With Three Optical Coherence Tomography Devices. Eye and Contact Lens, 2012, 38, 150-157.	0.8	20

Age-Related Changes in the Anterior Segment Biometry During Accommodation., 2015, 56, 3522.

20

#	Article	IF	CITATIONS
91	Altered Bulbar Conjunctival Microcirculation in Response to Contact Lens Wear. Eye and Contact Lens, 2017, 43, 95-99.	0.8	20
92	Role of optical coherence tomography angiography in the characterization of vascular network patterns of ocular surface squamous neoplasia. Ocular Surface, 2020, 18, 926-935.	2.2	20
93	Targeting CXCR7 improves the efficacy of breast cancer patients with tamoxifen therapy. Biochemical Pharmacology, 2018, 147, 128-140.	2.0	19
94	Visual Function and Disability Are Associated With Focal Thickness Reduction of the Ganglion Cell-Inner Plexiform Layer in Patients With Multiple Sclerosis. , 2019, 60, 1213.		19
95	Upper and Lower Tear Menisci After Laser In Situ Keratomileusis. Eye and Contact Lens, 2010, 36, 81-85.	0.8	18
96	Ultra-high resolution optical coherence tomography for monitoring tear meniscus volume in dry eye after topical cyclosporine treatment. Clinical Ophthalmology, 2012, 6, 933.	0.9	18
97	Quantitative analysis of conjunctival microvasculature imaged using optical coherence tomography angiography. Eye and Vision (London, England), 2019, 6, 5.	1.4	18
98	Msi2â€mediated MiR7aâ€1 processing repression promotes myogenesis. Journal of Cachexia, Sarcopenia and Muscle, 2022, 13, 728-742.	2.9	18
99	Evaluated Conjunctival Blood Flow Velocity in Daily Contact Lens Wearers. Eye and Contact Lens, 2018, 44, S238-S243.	0.8	17
100	Ultra high resolution optical coherence tomography in Boston type I keratoprosthesis. Journal of Ophthalmic and Vision Research, 2015, 10, 26.	0.7	17
101	Factors Affecting Microvascular Responses in the Bulbar Conjunctiva in Habitual Contact Lens Wearers. , 2018, 59, 4108.		16
102	Unique changes in the retinal microvasculature reveal subclinical retinal impairment in patients with systemic lupus erythematosus. Microvascular Research, 2020, 129, 103957.	1.1	16
103	Lid Wiper Microvascular Responses as an Indicator of Contact Lens Discomfort. American Journal of Ophthalmology, 2016, 170, 197-205.	1.7	15
104	Retinal nerve fiber layer (RNFL) integrity and its relations to retinal microvasculature and microcirculation in myopic eyes. Eye and Vision (London, England), 2018, 5, 25.	1.4	15
105	Associated risk factors in the early stage of diabetic retinopathy. Eye and Vision (London, England), 2019, 6, 23.	1.4	15
106	A review of functional slit lamp biomicroscopy. Eye and Vision (London, England), 2019, 6, 15.	1.4	15
107	Visualization of the Precorneal Tear Film Using Ultrahigh Resolution Optical Coherence Tomography in Dry Eye. Eye and Contact Lens, 2012, 38, 240-244.	0.8	14
108	Micrometer-Scale Contact Lens Movements Imaged by Ultrahigh-resolution Optical Coherence Tomography. American Journal of Ophthalmology, 2012, 153, 275-283.e1.	1.7	14

#	Article	IF	CITATIONS
109	Axial Biometry of the Entire Eye Using Ultra-Long Scan Depth Optical Coherence Tomography. American Journal of Ophthalmology, 2014, 157, 412-420.e2.	1.7	14
110	Functional slit lamp biomicroscopy metrics correlate with cardiovascular risk. Ocular Surface, 2019, 17, 64-69.	2.2	14
111	Discrimination of Diabetic Retinopathy From Optical Coherence Tomography Angiography Images Using Machine Learning Methods. IEEE Access, 2021, 9, 51689-51694.	2.6	14
112	Focal Thickness Reduction of the Ganglion Cell-Inner Plexiform Layer Best Discriminates Prior Optic Neuritis in Patients With Multiple Sclerosis. , 2019, 60, 4257.		13
113	A suitable silicosis mouse model was constructed by repeated inhalation of silica dust via nose. Toxicology Letters, 2021, 353, 1-12.	0.4	12
114	Detection of Magnetic Particles in Live DBA/2J Mouse Eyes Using Magnetomotive Optical Coherence Tomography. Eye and Contact Lens, 2010, 36, 346-351.	0.8	11
115	Effect of Punctal Occlusion on Tear Menisci in Symptomatic Contact Lens Wearers. Cornea, 2012, 31, 1014-1022.	0.9	11
116	The Relationship Between High-Order Aberration and Anterior Ocular Biometry During Accommodation in Young Healthy Adults. , 2017, 58, 5628.		11
117	Improving diabetic and hypertensive retinopathy with a medical food containing L-methylfolate: a preliminary report. Eye and Vision (London, England), 2019, 6, 21.	1.4	11
118	Altered birefringence of peripapillary retinal nerve fiber layer in multiple sclerosis measured by polarization sensitive optical coherence tomography. Eye and Vision (London, England), 2018, 5, 14.	1.4	10
119	Slit-Lamp–Adapted Ultra-High Resolution OCT for Imaging the Posterior Segment of the Eye. Ophthalmic Surgery Lasers and Imaging Retina, 2012, 43, 76-81.	0.4	10
120	Slitlamp Photography and Videography With High Magnifications. Eye and Contact Lens, 2015, 41, 391-397.	0.8	9
121	Retinal Tissue Perfusion in Patients with Multiple Sclerosis. Current Eye Research, 2019, 44, 1091-1097.	0.7	8
122	Improved conjunctival microcirculation in diabetic retinopathy patients with MTHFR polymorphisms after Ocufolinâ,,¢ Administration. Microvascular Research, 2020, 132, 104066.	1.1	8
123	In vivo quantification of cochlin in glaucomatous DBA/2J mice using optical coherence tomography. Scientific Reports, 2015, 5, 11092.	1.6	7
124	Retinal vessel density correlates with cognitive function in older adults. Experimental Gerontology, 2021, 152, 111433.	1.2	7
125	Tear Menisci after Overnight Contact Lens Wear. Optometry and Vision Science, 2011, 88, 1433-1438.	0.6	7
126	Loss of hypermethylated in cancer 1 (HIC1) promotes lung cancer progression. Cellular Signalling, 2019, 53, 162-169.	1.7	6

#	Article	IF	CITATIONS
127	Characterization of retinal microvasculature and its relations to cognitive function in older people after circuit resistance training. Experimental Gerontology, 2020, 142, 111114.	1.2	6
128	Effects of Ocufolin on retinal microvasculature in patients with mild non-proliferative diabetic retinopathy carrying polymorphisms of the MTHFR gene. BMJ Open Diabetes Research and Care, 2021, 9, e002327.	1.2	6
129	Wavefront Derived Refraction and Full Eye Biometry in Pseudophakic Eyes. PLoS ONE, 2016, 11, e0152293.	1.1	6
130	Necroptosis in pulmonary macrophages promotes silica-induced inflammation and interstitial fibrosis in mice. Toxicology Letters, 2022, 355, 150-159.	0.4	6
131	Vectorcardiographic Evaluation of Myocardial Infarct Size. Japanese Circulation Journal, 1998, 62, 473-478.	1.0	5
132	Targeted delivery of doxorubicin by lactobionic acid-modified laponite to hepatocarcinoma cells. Journal of Controlled Release, 2015, 213, e34.	4.8	5
133	Axial elongation measured by long scan depth optical coherence tomography during pilocarpine-induced accommodation in intraocular lens-implanted eyes. Scientific Reports, 2018, 8, 1981.	1.6	5
134	Long scan depth optical coherence tomography on imaging accommodation: impact of enhanced axial resolution, signal-to-noise ratio and speed. Eye and Vision (London, England), 2018, 5, 16.	1.4	5
135	Characterization of retinal microvasculature in acute non-arteritic anterior ischemic optic neuropathy using the retinal functional imager: a prospective case series. Eye and Vision (London,) Tj ETQq1 1 0	.78 143 14 r	gBѢ/Overlock
136	Microcirculation in the conjunctiva and retina in healthy subjects. Eye and Vision (London, England), 2019, 6, 11.	1.4	5
137	Conjunctival Vascular Adaptation Related to Ocular Comfort in Habitual Contact Lens Wearers. American Journal of Ophthalmology, 2020, 216, 99-109.	1.7	5
138	RETINAL TISSUE PERFUSION REDUCTION BEST DISCRIMINATES EARLY STAGE DIABETIC RETINOPATHY IN PATIENTS WITH TYPE 2 DIABETES MELLITUS. Retina, 2021, 41, 546-554.	1.0	5
139	Characterization of Soft Contact Lens Fitting Using Ultra-Long Scan Depth Optical Coherence Tomography. Journal of Ophthalmology, 2017, 2017, 1-13.	0.6	4
140	Comparison of Retinal Microvessel Blood Flow Velocities Acquired with Two Different Fields of View. Journal of Ophthalmology, 2017, 2017, 1-7.	0.6	4
141	The inter-visit variability of retinal blood flow velocity measurements using retinal function imager (RFI). Eye and Vision (London, England), 2018, 5, 31.	1.4	4
142	Inter-visit measurement variability of conjunctival vasculature and circulation in habitual contact lens wearers and non-lens wearers. Eye and Vision (London, England), 2019, 6, 10.	1.4	4
143	Characterization of the retinal vasculature in fundus photos using the PanOptic iExaminer system. Eye and Vision (London, England), 2020, 7, 46.	1.4	4
144	Conjunctival microvascular responses to anti-inflammatory treatment in patients with dry eye. Microvascular Research, 2020, 131, 104033.	1.1	4

#	Article	IF	CITATIONS
145	The Effect of Software Versions on the Measurement of Retinal Vascular Densities Using Optical Coherence Tomography Angiography. Current Eye Research, 2021, 46, 341-349.	0.7	4
146	Longitudinal Study of Retinal Structure, Vascular, and Neuronal Function in Patients With Relapsing-Remitting Multiple Sclerosis: 1-Year Follow-Up. Translational Vision Science and Technology, 2021, 10, 6.	1.1	4
147	Author Response: Human Accommodative Ciliary Muscle Configuration Changes Are Consistent With Schachar's Mechanism of Accommodation. , 2015, 56, 6076.		3
148	The Impact of Flap Creation Methods for Sub-Bowman's Keratomileusis (SBK) on the Central Thickness of Bowman's Layer. PLoS ONE, 2015, 10, e0124996.	1.1	3
149	Posterior Condyle Offset and Maximum Knee Flexion Following a Cruciate Retaining Total Knee Arthroplasty. Journal of Knee Surgery, 2019, 32, 146-152.	0.9	3
150	Wavelet Features of the Thickness Map of Retinal Ganglion Cell-Inner Plexiform Layer Best Discriminate Prior Optic Neuritis in Patients With Multiple Sclerosis. IEEE Access, 2020, 8, 221590-221598.	2.6	3
151	Focal alteration of the intraretinal layers in neurodegenerative disorders. Annals of Eye Science, 2020, 5, 8-8.	1.1	3
152	Conjunctival Vessels in Diabetes Using Functional Slit Lamp Biomicroscopy. Cornea, 2021, 40, 950-957.	0.9	3
153	Improved Retinal Microcirculation in Mild Diabetic Retinopathy Patients Carrying MTHFR Polymorphisms Who Received the Medical Food, Ocufolin®. Clinical Ophthalmology, 0, Volume 16, 1497-1504.	0.9	3
154	(CL-115)THE MEASUREMENT OF CORNEAL EPITHELIAL THICKNESS USING OPTICAL COHERENCE TOMOGRAPHY IN RESPONSE TO HYPOXIA INDUCED BY SOFT CONTACT LENS AND EYE CLOSURE. Optometry and Vision Science, 2000, 77, 170.	0.6	2
155	The Watery Eye. Current Allergy and Asthma Reports, 2011, 11, 192-196.	2.4	2
156	High resolution anterior segment optical coherence tomography of ocular surface lesions: a review and handbook. Expert Review of Ophthalmology, 2021, 16, 81-95.	0.3	2
157	Improvement of retinal tissue perfusion after circuit resistance training in healthy older adults. Experimental Gerontology, 2021, 146, 111210.	1.2	2
158	Retinal microvascular and neuronal function in patients with multiple sclerosis: 2-year follow-up. Multiple Sclerosis and Related Disorders, 2021, 56, 103314.	0.9	2
159	Advances in ophthalmic structural and functional measures in multiple sclerosis: do the potential ocular biomarkers meet the unmet needs?. Current Opinion in Neurology, 2021, 34, 97-107.	1.8	2
160	TOPOGRAPHICAL THICKNESS OF THE EPITHELIUM AND TOTAL CORNEA AFTER HYDROGEL AND PMMA CONTACT LENS WEAR WITH EYE CLOSURE Optometry and Vision Science, 2001, 78, 303.	0.6	1
161	CRF-Based Segmentation of Human Tear Meniscus Obtained with Optical Coherence Tomography. , 2007, , .		1
162	Ocular surface microvascular response and its relation to contact lens fitting and ocular comfort: an update of recent research. Australasian journal of optometry, The, 2021, 104, 661-671.	0.6	1

#	Article	IF	CITATIONS
163	Retinal microvascular density modifications during the water drinking test. European Journal of Ophthalmology, 2022, 32, 1602-1609.	0.7	1
164	Disruption of tear film and blink dynamics. , 2010, , 123-130.		1
165	Retinal vessel density correlates with cognitive function in older adults. Alzheimer's and Dementia, 2021, 17, .	0.4	0
166	Associations Between Lid Wiper Microvascular Responses, Lens Fit, and Comfort After One Day of Contact Lens Adaptation by Neophytes. Eye and Contact Lens, 2022, Publish Ahead of Print, .	0.8	0